

AN OPTIMIZATION-BASED ATOMISTIC-TO-CONTINUUM COUPLING METHOD*

DEREK OLSON[†], PAVEL B. BOCHEV[‡], MITCHELL LUSKIN[†], AND ALEXANDER V. SHAPEEV[†]

Abstract. We present a new optimization-based method for atomistic-to-continuum (AtC) coupling. The main idea is to cast the coupling of the atomistic and continuum models as a constrained optimization problem with virtual Dirichlet controls on the interfaces between the atomistic and continuum subdomains. The optimization objective is to minimize the error between the atomistic and continuum solutions on the overlap between the two subdomains, while the atomistic and continuum force balance equations provide the constraints. Splitting of the atomistic and continuum problems instead of blending them and their subsequent use as constraints in the optimization problem distinguishes our approach from the existing AtC formulations. We present and analyze the method in the context of a one-dimensional chain of atoms modeled using a linearized two-body next-nearest neighbor interactions.

1. Introduction. Atomistic-to-continuum (AtC) coupling methods aim to combine the efficiency of continuum models such as PDEs with the accuracy of the atomistic models necessary to resolve local features such as cracks or dislocations that can affect the global material behavior. Specifically, suppose that an atomistic model gives an accurate description of the true material behavior in a domain Ω , but that this model is prohibitively expensive to solve on the whole domain. The core of AtC formulations is to keep this model only where the fully atomistic description is required to accurately represent local features, while utilizing a more efficient continuum model in the rest of Ω . Existing AtC methods differ chiefly by the manner in which these models are joined together, which is also the main challenge in the AtC formulation.

To explain the main ideas we can consider a scenario where Ω is subdivided into an atomistic and a continuum subdomain, Ω_a and Ω_c , such that $\Omega_a \cup \Omega_c = \Omega$ and $\Omega_a \cap \Omega_c =: \Omega_o \neq \emptyset$. The overlap domain Ω_o is often referred to as the handshake or blending region. In an AtC method, we use the atomistic description on Ω_a and the continuum description on Ω_c . The problem then is how to couple the two different descriptions of the material over the overlap region, Ω_o .

Attempts at this problem thus far can be characterized as either energy-based, where a coupled energy is defined to be minimized; or force-based, where internal and external forces in Ω_a and Ω_c are equilibrated. In either case, the resulting AtC methods often involve some form of blending of the energy and/or the forces over the overlap region.

The extension of the Arlequin method [2] and quasicontinuum method [13, 17] are examples of blended energy AtC methods in which the continuum and atomistic energies are combined over Ω_o using a partition of unity. The blended functional is then minimized over Ω subject to a constraint expressing equality (in a suitable sense)

* Sandia National Laboratories is a multi-program laboratory managed and operated by Sandia Corporation, a wholly owned subsidiary of Lockheed Martin Corporation, for the U.S. Department of Energy's National Nuclear Security Administration under contract DE-AC04-94AL85000.

[†]University of Minnesota (`{olso4056,luskin,ashapeev}@umn.edu`). DO was supported by the Department of Defense (DoD) through the National Defense Science & Engineering Graduate Fellowship (NDSEG) Program. ML was supported in part by the NSF PIRE Grant OISE-0967140, DOE Award DE-SC0002085, and AFOSR Award FA9550-12-1-0187. AS was supported in part by the DOE Award DE-SC0002085.

[‡]Sandia National Laboratories, Numerical Analysis and Applications, P.O. Box 5800, MS 1320, Albuquerque, NM 87185-1320 (`pbboche@sandia.gov`).

of the atomistic and continuum displacements in Ω_o .

A standard way to define an AtC method using force blending is to start from the variational form of the atomistic and continuum models and blend the corresponding weak forms over Ω_o . We refer to [1] and [14] for investigations of blended force-based AtC formulations. A more extensive investigation of these and other AtC methods has been presented in [18].

In this paper, we formulate and analyze an optimization-based AtC method which differs significantly from the existing AtC approaches. The main idea is to cast AtC as a constrained optimization problem with virtual Dirichlet controls on the interfaces between the atomistic and continuum subdomains. The objective in this optimization problem is to minimize a suitable norm of the difference between the atomistic and continuum displacement fields over the overlap region Ω_o , while the atomistic and continuum force balance equations on Ω_a and Ω_c provide the constraints. Because we consider splitting the original problem over Ω into two subproblems over Ω_a and Ω_c , we also must impose some form of boundary condition on the two interfaces between Ω_a and Ω_c in order to have a well-posed problem. In the context of the optimization formulation, these boundary conditions act as Dirichlet controls. However, they are virtual, or artificial controls, because the boundaries on which they are imposed are artificial rather than actual domain boundaries.

While the AtC methods in [2, 7, 13, 14, 17] also involve a constrained optimization formulation, they differ fundamentally from the approach developed in this paper. Most notably, the former *minimize a blended energy functional* subject to constraints *forcing the equality* of the atomistic and continuum displacements over Ω_o . In contrast, our approach completely separates the two models and minimizes the discrepancy of the atomistic and continuum displacements in Ω_o subject to the two models acting independently in Ω_a and Ω_c . The reversal of the roles of the constraints and objectives in our approach, relative to blending methods, bears some important theoretical and computational advantages. It addresses the problem of blending two physical models over a shared spatial region by minimizing instead the mismatch of the deformations in the overlap region which is less restrictive on the overall formulation.

The use of optimization and control ideas for AtC further gives rise to a number of attractive theoretical and computational properties. For instance, we are able to infer key properties of the method from its atomistic and continuum constituencies, as illustrated in the proof of Lemma 4.2. This should be contrasted to the force-based quasicontinuum operator which fails to be stable in specific norms even though both atomistic and continuum force operators are stable [11].

The primary computational advantage of the proposed method is that code to implement the method can be built upon preexisting code for solving individual atomistic and continuum problems. Since the core feature is minimizing the difference between solutions of an atomistic model and a continuum model, all that is required is a linking program between the two algorithms which carries out the optimization.

Our AtC work follows a number of previous efforts exploring the use of optimization and control ideas for the design of numerical methods [3–5, 15, 16]. Conceptually, our approach is closest to the virtual control techniques for heterogeneous domain decomposition developed in [12]. In that setting, both domains are modeled using a local, continuum (PDE) model, whereas here we are concerned solely with coupling a nonlocal atomistic model with a local continuum model.

Since the main goal of this paper is to demonstrate the application of optimization and control ideas to AtC, we formulate and analyze our method using a linearized

Lennard-Jones type atomistic model [8, 10, 19]. For completeness, we review this model in Section 2. We present the new method in Section 3 and analyze its error in Section 4. Section 5 summarizes our conclusions.

2. Preliminaries. This section establishes the notation and defines the model atomistic problem. Application of the Cauchy-Born rule [10] to this problem yields the continuum formulation.

2.1. The atomistic model. We consider a chain of $N + 1$ atoms with reference (undeformed) positions X_i , $i = 0, \dots, N$. The atomic positions in the deformed configuration are x_i , $i = 0, \dots, N$, and $u_i = x_i - X_i$ is the displacement of atom i . We assume each atom interacts with its first and second neighbors through a linearized Lennard-Jones type potential. Thus, we can effectively think of atoms interacting with first and second neighbors via linear springs with spring constants $k_1 > 0$ and k_2 , respectively, and equilibrium lengths ℓ and 2ℓ , respectively. For the linearization of typical interatomic potentials such as Lennard-Jones, the second neighbor spring constant satisfies $k_2 < 0$ [10] and so is not a physical spring, but we will assume $k_2 < 0$ in the following. We also assume nearest neighbor interactions dominate second neighbor interactions with the hypothesis

$$k_1 + 4k_2 > 0, \quad (2.1)$$

which is also necessary and sufficient for the stability of the atomistic problem [11] we consider below. For simplicity, we set the lattice parameter $\ell = 1$.

Under these assumptions, the computational domain is $\Omega := [0, N] \cap \mathbb{Z}$, and the lattice displacements $u = \{u_0, \dots, u_N\}$ are elements of the space

$$\mathcal{U} := \{u : \Omega \rightarrow \mathbb{R}\}$$

with inner product $(\cdot, \cdot)_{\ell^2(\Omega)}$ and norm $\|\cdot\|_{\ell^2(\Omega)} = (\cdot, \cdot)_{\ell^2(\Omega)}^{1/2}$. The left and right “boundaries” of Ω are $\Gamma^- = \{0, 1\}$ and $\Gamma^+ = \{N-1, N\}$, respectively¹, and $\Omega^\circ = [2, N-2] \cap \mathbb{Z}$ is the interior. The size of a domain is $|\cdot|$, for example, $|\Omega| = (N+1)$ and $|\Omega^\circ| = N-3$.

The potential energy of the lattice is the sum of first and second neighbor interactions

$$\mathcal{E}^a(u) := \sum_{i=0}^{N-1} \frac{k_1}{2} (u_{i+1} - u_i)^2 + \sum_{i=1}^{N-1} \frac{k_2}{2} (u_{i+1} - u_{i-1})^2. \quad (2.2)$$

We impose homogeneous Dirichlet boundary conditions by fixing the atoms in Γ^- and Γ^+ . The corresponding homogeneous space of admissible displacements is then

$$\mathcal{U}_0 := \{u \in \mathcal{U} : u = 0 \text{ on } \Gamma^- \cup \Gamma^+\}.$$

We assume that a dead load external force, $f \in \mathcal{U}_0$, is applied at each atom site resulting in a total energy of

$$\mathcal{E}_a^{tot}(u) = \mathcal{E}^a(u) - (f, u)_{\ell^2(\Omega)}. \quad (2.3)$$

An equilibrium configuration of the lattice under the dead load is then given by

$$\tilde{u}^a = \arg \min_{u \in \mathcal{U}_0} \mathcal{E}_a^{tot}(u). \quad (2.4)$$

¹The reason for fixing two boundary atoms is to ensure all unconstrained atoms have a full set of neighbors to interact with and avoid boundary defects

The Euler-Lagrange equations

$$\frac{\partial \mathcal{E}_a^{tot}(\tilde{u}^a)}{\partial u_i} = 0, \quad i \in \Omega^\circ, \quad (2.5)$$

for (2.4) give the force balance constraints at each internal atom. We express these constraints using the finite difference operators $\Delta_1, \Delta_2 : \mathcal{U}_0 \rightarrow \mathcal{U}_0$ defined by

$$\begin{aligned} (\Delta_1 u)_i &= u_{i-1} - 2u_i + u_{i+1}, \quad i \in \Omega^\circ, \\ (\Delta_2 u)_i &= u_{i-2} - 2u_i + u_{i+2}, \quad i \in \Omega^\circ. \end{aligned}$$

From (2.5), the internal force at site i for $i \in \Omega^\circ$ equals $(k_1 \Delta_1 u + k_2 \Delta_2 u)_i$. Thus, the necessary conditions for the equilibrium of the atomistic system are

$$-(k_1 \Delta_1 \tilde{u}^a + k_2 \Delta_2 \tilde{u}^a)_i = f_i, \quad i \in \Omega^\circ, \quad (2.6)$$

$$\tilde{u}_i^a = 0, \quad i \in \Gamma^- \cup \Gamma^+. \quad (2.7)$$

The system of linear algebraic equations (2.6)–(2.7) represents the fully atomistic problem, which we write compactly as:

$$\text{find } \tilde{u}^a \in \mathcal{U}_0 \text{ such that } A\tilde{u}^a = f, \quad (2.8)$$

where $A := -k_1 \Delta_1 - k_2 \Delta_2$.

2.2. The continuum model. To derive the continuum (local) model, we use the Cauchy-Born rule $u_i \approx 1/2(u_{i+1} + u_{i-1})$; see [18], to approximate the second neighbor interactions by first neighbor interactions

$$(u_{i+1} - u_{i-1})^2 \approx 2(u_{i+1} - u_i)^2 + 2(u_i - u_{i-1})^2. \quad (2.9)$$

Substitution of the Cauchy-Born approximation (2.9) into the atomistic energy (2.2) yields the continuum potential energy

$$\mathcal{E}^c = \frac{1}{2} \sum_{i=0}^{N-1} k_c (u_{i+1} - u_i)^2 - k_2 (u_1 - u_0)^2 - k_2 (u_N - u_{N-1})^2, \quad (2.10)$$

where $k_c = k_1 + 4k_2$. We note that a surface Cauchy-Born correction is not needed for (2.10) since we are assuming that $u_i = 0$ for $i \in \Gamma^- \cup \Gamma^+$.

We now define the total continuum energy under a force $f \in \mathcal{U}_0$ as

$$\mathcal{E}_c^{tot}(u) = \mathcal{E}^c(u) - (f, u)_{\ell^2(\Omega)}. \quad (2.11)$$

An equilibrium configuration of the continuum model minimizes the total energy:

$$\tilde{u}^c = \arg \min_{u \in \mathcal{U}_0} \mathcal{E}_c^{tot}(u). \quad (2.12)$$

The Euler-Lagrange equations for (2.12) are given by

$$-(k_c \Delta_1 \tilde{u}^c)_i = f_i, \quad i \in \Omega^\circ, \quad (2.13)$$

$$\tilde{u}_i^c = 0, \quad i \in \Gamma^- \cup \Gamma^+. \quad (2.14)$$

The system of linear algebraic equations (2.13)–(2.14) represents the continuum problem. Setting $C = -k_c \Delta_1$, this system assumes the form:

$$\text{find } \tilde{u}^c \in \mathcal{U}_0 \text{ such that } C\tilde{u}^c = f. \quad (2.15)$$

2.3. The continuum modeling error. The error in the approximation of the atomistic solution by the continuum solution is given by the following proposition.

PROPOSITION 2.1. *There exists a fixed constant c_0 , independent of N and \tilde{u}^a , such that*

$$\|\tilde{u}^a - \tilde{u}^c\|_{\ell^2(\Omega)} \leq c_0 N^2 \|\Delta_1^2 \tilde{u}^a\|_{\ell^2(\Omega)}. \quad (2.16)$$

Proof. To estimate the continuum modeling error, we observe that

$$A - C = -(k_1 \Delta_1 + k_2 \Delta_2) + (k_1 + 4k_2) \Delta_1 = -k_2 (\Delta_2 - 4\Delta_1) = -k_2 \Delta_1^2.$$

Now C is just the 1D discrete Laplacian on Ω with homogeneous Dirichlet boundary conditions at atom sites 1 and $N - 1$. So, the minimum eigenvalue for C is $\lambda_1 = 4k_c \sin^2\left(\frac{\pi}{2(n+1)}\right)$ where $n = N - 3$ is the number of unconstrained atoms. Using that $\tilde{u}^a - \tilde{u}^c = 0$ at atoms 1 and $N - 1$ implies $C\tilde{u}^c = f = A\tilde{u}^a$, which yields the following bound:

$$\begin{aligned} \|\tilde{u}^a - \tilde{u}^c\|_{\ell^2(\Omega)} &\leq \|C^{-1}\|_{\ell^2(\Omega)} \cdot \|C(\tilde{u}^a - \tilde{u}^c)\|_{\ell^2(\Omega)} \\ &= \|C^{-1}\|_{\ell^2(\Omega)} \cdot \|C\tilde{u}^a - A\tilde{u}^a\|_{\ell^2(\Omega)} \\ &= |k_2| \|C^{-1}\|_{\ell^2(\Omega)} \cdot \|\Delta_1^2 \tilde{u}^a\|_{\ell^2(\Omega)} \\ &= \frac{|k_2|}{4k_c \sin^2\left(\frac{\pi}{2(n+1)}\right)} \|\Delta_1^2 \tilde{u}^a\|_{\ell^2(\Omega)} \leq c_0 N^2 \|\Delta_1^2 \tilde{u}^a\|_{\ell^2(\Omega)}. \end{aligned}$$

□

3. Optimization-based AtC formulation. As with any AtC formulation, we begin by splitting Ω into atomistic, continuum, and overlap regions

$$\Omega_a = [0, L] \cap \mathbb{Z}, \quad \Omega_c = [K, N] \cap \mathbb{Z}, \quad \Omega_o = \Omega_a \cap \Omega_c = [K, L] \cap \mathbb{Z},$$

where $0 < K < L < N$. The strict interiors of these domains are

$$\Omega_a^\circ = [2, L - 2] \cap \mathbb{Z}, \quad \Omega_c^\circ = [K + 2, N - 2] \cap \mathbb{Z}, \quad \Omega_o^\circ = \Omega_a^\circ \cap \Omega_c^\circ = [K + 2, L - 2] \cap \mathbb{Z},$$

and their boundaries are

$$\begin{aligned} \Gamma_a^- &= \{0, 1\} \quad \text{and} \quad \Gamma_a^+ = \{L - 1, L\}, \\ \Gamma_c^- &= \{K, K + 1\} \quad \text{and} \quad \Gamma_c^+ = \{N - 1, N\}, \\ \Gamma_o^- &= \{K, K + 1\} \quad \text{and} \quad \Gamma_o^+ = \{L - 1, L\}. \end{aligned}$$

Here and in the remainder of the paper, we find it convenient to use modified Vinogradov notation where the implied constant is independent of the parameters K, L , and N . Thus, $X \gtrsim Y$ means there is a positive constant c such that $X \geq cY$ with c independent of K, L , and N .

Recall that the main objective of an AtC method is a stable, accurate, and efficient approximation of the lattice displacements by using the atomistic model on Ω_a , employing the continuum approximation on Ω_c , and accurately merging them together on Ω_o . It follows that the efficiency of AtC methods hinges on the assumption that the atomistic region is small compared to the continuum region. On the other

hand, it is intuitively clear that a stable and accurate AtC method requires some conditions on the size of Ω_o . These assumptions are pivotal to our analysis and we formalize them below.

ASSUMPTION A. *There exists a real number $p > 1$ such that*

$$L \lesssim N^{1/p}.$$

ASSUMPTION B. *There exists a real number γ , $\frac{3}{L} < \gamma < 1$, such that*

$$\frac{L - K}{L} = \gamma.$$

In other words, we assume that $|\Omega_a| \lesssim |\Omega|^{1/p}$ and $|\Omega_o| = \gamma|\Omega_a|$ is such that $|\Omega_o| > 3$, i.e., the overlap region's size is at least twice the size of the interaction range; see Fig. 3.1. The assumption that γ is constant means the ratio of the overlap width to the size of the atomistic region is constant, or equivalently, that the ratio of K to L is constant.

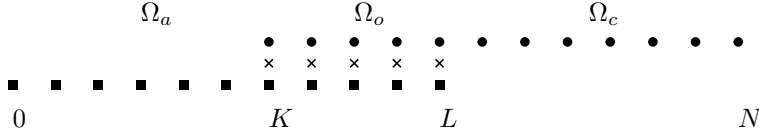


FIG. 3.1. *Decomposition of Ω . Squares are in the atomistic region Ω_a , circles are in the continuum region Ω_c , and crosses are in the overlap region Ω_o .*

We formulate the optimization-based AtC method in two steps. The first step defines independent atomistic and continuum subproblems on Ω_a and Ω_c , respectively, whereas the second step merges these problems by minimizing the mismatch of their solutions on Ω_o . To describe the first step, we introduce the spaces

$$\begin{aligned} \mathcal{U}_a &:= \{u : \Omega_a \rightarrow \mathbb{R} \mid u = 0 \text{ on } \Gamma_a^-\}, \\ \mathcal{U}_{a,0} &:= \{u : \Omega_a \rightarrow \mathbb{R} \mid u = 0 \text{ on } \Gamma_a^- \cup \Gamma_a^+\}, \\ \mathcal{U}_c &:= \{u : \Omega_c \rightarrow \mathbb{R} \mid u = 0 \text{ on } \Gamma_c^+\}, \\ \mathcal{U}_{c,0} &:= \{u : \Omega_c \rightarrow \mathbb{R} \mid u = 0 \text{ on } \Gamma_c^- \cup \Gamma_c^+\}, \end{aligned}$$

for the subdomain displacements and the “trace” spaces

$$\Lambda_a = \{w : \Gamma_a^+ \rightarrow \mathbb{R}\} \quad \text{and} \quad \Lambda_c = \{w : \Gamma_c^- \rightarrow \mathbb{R}\} \quad (3.1)$$

for the displacement values on the artificial domain boundaries Γ_a^+ and Γ_c^- . We denote the standard ℓ^2 inner product and norm on these spaces by $(\cdot, \cdot)_{\ell^2(\sigma)}$ and $\|\cdot\|_{\ell^2(\sigma)}$, where σ stands for the appropriate domain under consideration. The trace spaces provide the boundary conditions on Γ_a^+ and Γ_c^- necessary to formulate well-posed atomistic and continuum problems on Ω_a and Ω_c .

Let A_a and f^a be the restrictions of A and f to the interior Ω_a° . Likewise, let C_c and f^c denote the restrictions of C and f to the interior Ω_c° . The local nature of the continuum subdomain operator C_c necessitates the need for only a single boundary constraint on Γ_c^- whereas the atomistic subdomain operator A_a requires two constraints on Γ_a^+ . For this reason, when referring to the continuum model, we adjust the definitions of Ω_c , Ω_c° , Γ_c^- , and Γ_c^+ to be

$$\Omega_c = [K, N - 1] \cap \mathbb{Z}, \quad \Omega_c^\circ = [K + 1, N - 2] \cap \mathbb{Z}, \quad \Gamma_c^- = \{K\}, \quad \Gamma_c^+ = \{N - 1\},$$

with analogous changes made to overlap boundaries and interiors and the displacement and trace spaces. Thus, the left, artificial boundary and the right, true boundary of the continuum region are single atoms. The continuum displacement at atom N is zero since this is a true boundary condition of the original problem. To simplify notation in upcoming computations, we set $\bar{N} := N - 1$; see (3.2).

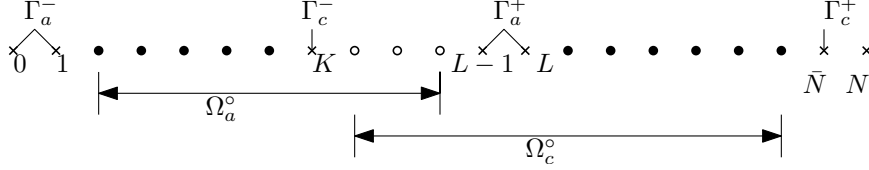


FIG. 3.2. Trace spaces and interiors of Ω_a, Ω_c . The interior of Ω_o is depicted with open circles.

We define the atomistic subproblem as a restriction of (2.8) to Ω_a with inhomogeneous boundary conditions at the artificial atomistic boundary Γ_a^+ , i.e., given $\theta^a \in \Lambda^a$ we seek $u^a \in \mathcal{U}_a$ such that

$$\begin{cases} A_a u^a = f^a & \text{on } \Omega_a^\circ \\ u^a = \theta^a & \text{on } \Gamma_a^+ \end{cases}. \quad (3.2)$$

Similarly, the continuum subproblem is a restriction of (2.15) to Ω_c with inhomogeneous boundary condition at the artificial continuum boundary Γ_c^- : given $\theta^c \in \Lambda_c$ we seek $u^c \in \mathcal{U}_c$ such that

$$\begin{cases} C_c u^c = f^c & \text{on } \Omega_c^\circ \\ u^c = \theta^c & \text{on } \Gamma_c^- \end{cases}. \quad (3.3)$$

Thanks to the boundary conditions prescribed on the artificial boundaries, the subdomain problems (3.2)–(3.3) are well-posed and can be solved for any given θ^a and θ^c . However, because θ^a and θ^c are unknown, the solutions to (3.2) and (3.3) cannot yet be determined.

The second step in the formulation of our AtC method is the merging of (3.2) and (3.3) into a single well-posed problem for the unknown states u^a and u^c , and the unknown boundary conditions θ^a and θ^c . Intuitively, we desire that

$$\theta^c \approx u^a \text{ on } \Gamma_c^-, \quad \theta^a \approx u^c \text{ on } \Gamma_a^+, \quad \text{and} \quad u^a \approx u^c \text{ in } \Omega_o^\circ. \quad (3.4)$$

In many hybrid AtC methods these, or similar conditions, are used to constrain the hybrid force balance equations or the minimization of a hybrid energy functional; see e.g., [2, 7, 14]. However, there is no canonical way of enforcing strong or weak type equality of fundamentally different atomistic and continuum solution states.

The cornerstone of our optimization-based AtC approach is to view (3.4) as the optimization objective rather than as the constraint. Specifically, in the context of our model problem, the quantity

$$\|u^a - u^c\|_{\ell^2(\Omega_o)}^2 = \|u^a - \theta^c\|_{\ell^2(\Lambda_c)}^2 + \|u^a - u^c\|_{\ell^2(\Omega_o^\circ)}^2 + \|u^c - \theta^a\|_{\ell^2(\Lambda_a)}^2 \quad (3.5)$$

provides a notion of an artificial “mismatch” energy between the solutions of (3.2) and (3.3) in the overlap region. Instead of forcing this energy to be exactly zero, which does

not yield a problem with a solution, we seek to minimize it subject to the atomistic and continuum force balance equations (3.2) and (3.3) holding independently in Ω_a and Ω_c . Succinctly, our new AtC formulation is the following constrained optimization problem:

$$\min_{\{u^a, u^c, \theta^a, \theta^c\}} \frac{1}{2} \|u^a - u^c\|_{\ell_2(\Omega_o)}^2 \text{ s.t. } \begin{cases} A_a u^a = f^a & \text{on } \Omega_a^\circ \\ u^a = \theta^a & \text{on } \Gamma_a^+ \end{cases}, \quad \begin{cases} C_c u^c = f^c & \text{on } \Omega_c^\circ \\ u^c = \theta^c & \text{on } \Gamma_c^- \end{cases}. \quad (3.6)$$

In the language of constrained optimization, the functions $u^a \in \mathcal{U}_a$ and $u^c \in \mathcal{U}_c$ are the *states*, and the artificial boundary conditions $\theta^a \in \Lambda_a$ and $\theta^c \in \Lambda_c$ are the *controls*. The purpose of the controls is to allow the states to adjust so as to provide the smallest possible value of the objective while still satisfying the constraints. In the context of (3.6), θ^a and θ^c are *virtual boundary* controls, as the boundaries Γ_a^+ and Γ_c^- are an artifact of the domain decomposition into atomistic and continuum parts.

We shall show below that the optimization problem (3.6) is well-posed. But before investigating this, we show the optimization-based AtC formulation (3.6) satisfies a patch test criterion.

3.1. Patch Test Consistency. The bane of all atomistic-to-continuum coupling mechanisms is the existence of nonphysical ghost forces arising on the interface of the continuum and atomistic regions [9, 20]. The patch test is a well-known test for determining the existence of ghost forces by checking whether a uniform strain is an equilibrium solution to the proposed method on a perfect lattice under zero external forces [18, 20]. As with force-based methods, the optimization formulation (3.6) is patch test consistent by design. Indeed, if we replace the homogeneous Dirichlet boundary conditions by the inhomogeneous boundary conditions

$$u_0^a = 0, \quad u_1^a = F \quad \text{and} \quad u_{N-1}^c = (N-1)F, \quad u_N^c = NF,$$

where $F > 0$ defines a macroscopic displacement gradient, and if we take $f^a \equiv 0$, $f^c \equiv 0$, then it is straightforward to verify that (3.6) has a minimum of 0 achieved when $u_i^a = iF$ and $u_i^c = iF$. This is due to the fact that both atomistic and continuum operators are patch test consistent individually.

3.2. Well-Posedness. To establish that the optimization-based AtC formulation (3.6) is well-posed, we switch to the reduced space form of the optimization problem, which requires the elimination of the states from (3.6). In our case, this task is trivial because for any pair of virtual controls $\{\theta^a, \theta^c\} \in \Lambda_a \times \Lambda_c$ the constraints

$$\begin{cases} A_a u^a = f^a & \text{on } \Omega_a^\circ, \\ u^a = \theta^a & \text{on } \Gamma_a^+, \end{cases} \quad \text{and} \quad \begin{cases} C_c u^c = f^c & \text{on } \Omega_c^\circ, \\ u^c = \theta^c & \text{on } \Gamma_c^-, \end{cases} \quad (3.7)$$

have unique solutions $u^a = u^a(\theta^a) \in \mathcal{U}_a$ and $u^c = u^c(\theta^c) \in \mathcal{U}_c$. Using these solutions in (3.6) transforms the latter into an equivalent unconstrained minimization problem

$$\min_{\{\theta^a, \theta^c\} \in \Lambda_a \times \Lambda_c} \frac{1}{2} \|u^a(\theta^a) - u^c(\theta^c)\|_{\ell_2(\Omega_o)}^2. \quad (3.8)$$

This problem, in terms of the virtual controls only, is the reduced space form of (3.6). We analyze (3.8) following the strategy in Gervasio et al. [12]. Specifically, for any given $\{\theta^a, \theta^c\} \in \Lambda_a \times \Lambda_c$ we split the solutions of the constraint equations (3.7) as

$$u^a(\theta^a) = v^a(\theta^a) + u^{a,0} \quad \text{and} \quad u^c(\theta^c) = v^c(\theta^c) + u^{c,0} \quad (3.9)$$

where the homogeneous components $u^{a,0} \in \mathcal{U}_{a,0}$ and $u^{c,0} \in \mathcal{U}_{c,0}$ solve

$$A_a u^{a,0} = f^a \quad \text{and} \quad C_c u^{c,0} = f^c, \quad (3.10)$$

respectively, whereas $v^a(\theta^a) \in \mathcal{U}_a$ and $v^c(\theta^c) \in \mathcal{U}_c$ solve

$$\begin{cases} A_a v^a = 0 & \text{on } \Omega_a^\circ \\ v^a = \theta^a & \text{on } \Gamma_a^+ \end{cases} \quad \text{and} \quad \begin{cases} C_c v^c = 0 & \text{on } \Omega_c^\circ \\ v^c = \theta^c & \text{on } \Gamma_c^- \end{cases}, \quad (3.11)$$

respectively. We will prove the following stability result for (3.11) in Appendix A.

LEMMA 3.1. *For any $\{\theta^a, \theta^c\} \in \Lambda_a \times \Lambda_c$, the solutions $v^a(\theta^a)$ and $v^c(\theta^c)$ to (3.11) satisfy the bounds*

$$\begin{aligned} \|v^a(\theta^a)\|_{\ell^2(\Omega_a)}^2 &\lesssim L \|\theta^a\|_{\ell^2(\Gamma_a^+)}^2, \\ \|v^c(\theta^c)\|_{\ell^2(\Omega_c)}^2 &\leq (N - K) \|\theta^c\|_{\ell^2(\Gamma_c^-)}^2 \end{aligned} \quad (3.12)$$

REMARK 3.1. *The bounds (3.12) continue to hold when we take homogeneous Dirichlet boundary conditions on Γ_a^+ and Γ_c^- in (3.11) and inhomogeneous boundary conditions on Γ_a^- and Γ_c^+ by replacing Γ_a^+ with Γ_a^- and Γ_c^- with Γ_c^+ .*

Using the decomposition (3.9), the reduced space problem (3.8) assumes the form

$$\begin{aligned} \min_{\{\theta^a, \theta^c\} \in \Lambda_a \times \Lambda_c} & \frac{1}{2} \|v^a(\theta^a) - v^c(\theta^c)\|_{\ell^2(\Omega_o)}^2 + (v^a(\theta^a) - v^c(\theta^c), u^{a,0} - u^{c,0})_{\ell^2(\Omega_o)} \\ & + \frac{1}{2} \|u^{a,0} - u^{c,0}\|_{\ell^2(\Omega_o)}^2. \end{aligned} \quad (3.13)$$

The following result is key to proving that the reduced space problem (3.8), respectively (3.13), has a unique minimizer.

THEOREM 3.2. *The form*

$$\langle \{\theta^a, \theta^c\}, \{\mu^a, \mu^c\} \rangle := (v^a(\theta^a) - v^c(\theta^c), v^a(\mu^a) - v^c(\mu^c))_{\ell^2(\Omega_o)} \quad (3.14)$$

defines an inner product on $\Lambda_a \times \Lambda_c$.

Proof. The proof follows from the inequality (4.15) in Lemma 4.2.

□

Theorem 3.2 allows us to recast the reduced space problem (3.13) as

$$\begin{aligned} \min_{\{\theta^a, \theta^c\} \in \Lambda_a \times \Lambda_c} & \frac{1}{2} \|\{\theta^a, \theta^c\}\|_{\ell^*(\Lambda_a \times \Lambda_c)}^2 + (v^a(\theta^a) - v^c(\theta^c), u^{a,0} - u^{c,0})_{\ell^2(\Omega_o)} \\ & + \frac{1}{2} \|u^{a,0} - u^{c,0}\|_{\ell^2(\Omega_o)}^2, \end{aligned} \quad (3.15)$$

where $\|\cdot\|_{\ell^*(\Lambda_a \times \Lambda_c)}$ is the norm induced by (3.14). The necessary optimality condition (Euler-Lagrange equation) for (3.15) is the following variational equation: find $\{\theta^a, \theta^c\} \in \Lambda_a \times \Lambda_c$ such that

$$\langle \{\theta^a, \theta^c\}, \{\mu^a, \mu^c\} \rangle = - (u^{a,0} - u^{c,0}, v^a(\mu^a) - v^c(\mu^c))_{\ell^2(\Omega_o)} \quad (3.16)$$

for all $\{\mu^a, \mu^c\} \in (\Lambda_a \times \Lambda_c)$. Theorem 3.2 and the Riesz representation theorem imply that (3.16) has a unique solution, thereby establishing the well-posedness of the reduced space problem (3.13).

REMARK 3.3. *There are two principal pathways for the analysis and the numerical solution of the constrained optimization problem (3.6). The first one, which we adopt in this paper, relies on the strictly convex reduced space problem (3.8) and its equivalent forms (3.13) and (3.15). In this case the practical implementation of the AtC method involves the solution of the strongly coercive Euler-Lagrange equation (3.16), followed by the recovery of the atomistic and continuum states from the virtual controls.*

The second pathway relies on Lagrange multipliers to enforce the constraints in (3.6) and yields a saddle-point optimization problem. The latter can be analyzed using the Brezzi's theory [6], while implementation of the AtC method then requires the solution of a weakly-coercive, mixed-type optimality system. We note that showing the conditions of the Brezzi theory is essentially equivalent to showing the well-posedness of the reduced space problem.

REMARK 3.4. *Let A_c be the restriction of A to the continuum subdomain Ω_c . Substituting A_c for C_c in (3.6) yields a constrained optimization formulation that is equivalent to the global atomistic problem (2.8). The corresponding reduced space problem and its Euler-Lagrange equation differ from (3.15) and (3.16) only by the use of the atomistic operator A_c instead of C_c . As a result, the variational problem (3.16) can be thought of as resulting from a modification of the bilinear form associated to the original problem very similar to a nonconforming finite element method.*

4. Consistency and Error Analysis. This section analyzes the error between the true solution \tilde{u}^a to the atomistic problem (2.6) and the solution of the optimization-based AtC formulation (3.6).

To proceed with our analysis, let $\{\theta_{op}^a, \theta_{op}^c\} \in \Lambda_a \times \Lambda_c$ denote the optimal solution of the reduced space problem (3.15) or, what is the same—the solution of the Euler-Lagrange equation (3.16). The optimal solution of the full problem (3.6) is then given by $\{u_{op}^a, u_{op}^c, \theta_{op}^a, \theta_{op}^c\}$, where

$$u_{op}^a = v^a(\theta_{op}^a) + u^{a,0} \quad \text{and} \quad u_{op}^c = v^c(\theta_{op}^c) + u^{c,0}.$$

These are the optimal states. Using these states we define the AtC approximation to \tilde{u}^a as

$$u^{atc} := \begin{cases} u_{op}^a & \text{in } \Omega_a, \\ u_{op}^c & \text{in } \Omega_c \setminus \Omega_o. \end{cases} \quad (4.1)$$

For the error analysis, it is convenient to express the approximate AtC solution as

$$u^{atc} = P(\{\theta_{op}^a, \theta_{op}^c\}),$$

where the affine operator, $P : \Lambda_a \times \Lambda_c \rightarrow \mathcal{U}_0$, is defined by

$$P(\{\mu^a, \mu^c\}) := \begin{cases} u^{a,0} + v^a(\mu^a) & \text{in } \Omega_a, \\ u^{c,0} + v^c(\mu^c) & \text{in } \Omega_c \setminus \Omega_o, \end{cases} \quad \forall \{\mu^a, \mu^c\} \in \Lambda_a \times \Lambda_c. \quad (4.2)$$

Thus, the error of the AtC approximation (4.1) is

$$\|\tilde{u}^a - u^{atc}\|_{\ell^2(\Omega)} = \|\tilde{u}^a - P(\{\theta_{op}^a, \theta_{op}^c\})\|_{\ell^2(\Omega)}. \quad (4.3)$$

To analyze (4.3) it is advantageous to split P into a linear part, Q , and constant term, U^0 , dependent only on the homogeneous data, i.e., $P = Q + U^0$ where

$$Q(\{\mu^a, \mu^c\}) := \begin{cases} v^a(\mu^a) & \text{in } \Omega_a, \\ v^c(\mu^c) & \text{in } \Omega_c \setminus \Omega_o, \end{cases} \quad \text{and} \quad U^0 := \begin{cases} u^{a,0} & \text{in } \Omega_a, \\ u^{c,0} & \text{in } \Omega_c \setminus \Omega_o. \end{cases}$$

We also introduce the trace operator $r : \mathcal{U}_0 \mapsto \Lambda_a \times \Lambda_c$ such that

$$r(u) := \left\{ \begin{pmatrix} u_{L-1} \\ u_L \end{pmatrix}, (u_K) \right\} := \{r^a(u), r^c(u)\} \quad \forall u \in \mathcal{U}_0. \quad (4.4)$$

Because $r^a(\tilde{u}^a)$ contains the exact values of the atomistic solution, it follows that

$$\tilde{u}^a|_{\Omega_a} = v^a(r^a(\tilde{u}^a)) + u^{a,0}. \quad (4.5)$$

We define the continuum lifting of the exact atomistic trace on Λ_c as

$$u^c := v^c(r^c(\tilde{u}^a)) + u^{c,0}. \quad (4.6)$$

It is a matter of unraveling these definitions to see that

$$P(r(\tilde{u}^a)) = P(\{r^a(\tilde{u}^a), r^c(\tilde{u}^a)\}) = \begin{cases} \tilde{u}^a & \text{in } \Omega_a, \\ u^c & \text{in } \Omega_c \setminus \Omega_o. \end{cases} \quad (4.7)$$

To estimate the AtC approximation error we split (4.3) into two parts:

$$\begin{aligned} & \|\tilde{u}^a - P(\{\theta_{op}^a, \theta_{op}^c\})\|_{\ell^2(\Omega)} \\ &= \|\tilde{u}^a - P(r(\tilde{u}^a)) + P(r(\tilde{u}^a)) - P(\{\theta_{op}^a, \theta_{op}^c\})\|_{\ell^2(\Omega)} \\ &\leq \|\tilde{u}^a - P(r(\tilde{u}^a))\|_{\ell^2(\Omega)} + \|Qr(\tilde{u}^a) + U^0 - Q\{\theta_{op}^a, \theta_{op}^c\} - U^0\|_{\ell^2(\Omega)} \\ &= \|\tilde{u}^a - P(r(\tilde{u}^a))\|_{\ell^2(\Omega)} + \|Q(r(\tilde{u}^a) - \{\theta_{op}^a, \theta_{op}^c\})\|_{\ell^2(\Omega)} \\ &\leq \|\tilde{u}^a - P(r(\tilde{u}^a))\|_{\ell^2(\Omega)} + \|Q\| \cdot \|r(\tilde{u}^a) - \{\theta_{op}^a, \theta_{op}^c\}\|_{\ell^*(\Lambda_a \times \Lambda_c)}, \end{aligned} \quad (4.8)$$

where $\|\cdot\|_{\ell^*(\Lambda_a \times \Lambda_c)}$ is the norm induced by (3.14) and

$$\|Q\| = \sup_{\{\mu^a, \mu^c\} \in \Lambda_a \times \Lambda_c} \frac{\|Q(\{\mu^a, \mu^c\})\|_{\ell^2(\Omega)}}{\|\{\mu^a, \mu^c\}\|_{\ell^*(\Lambda_a \times \Lambda_c)}}. \quad (4.9)$$

The first term in (4.8) is the consistency error of the operator P . Using (4.7)

$$\|\tilde{u}^a - P(r(\tilde{u}^a))\|_{\ell^2(\Omega)} = \|\tilde{u}^a - u^c\|_{\ell^2(\Omega_c \setminus \Omega_o)}, \quad (4.10)$$

i.e., the consistency error is confined to the purely continuum region. The second term is proportional, up to a factor of $\|Q\|$, to the approximation error² in the solution of the reduced space problem (3.13). We proceed with an estimate of the approximation error, followed by a bound on the operator norm $\|Q\|$.

LEMMA 4.1. *Let \tilde{u}^a solve (2.6) and $\{\theta_{op}^a, \theta_{op}^c\}$ be the minimizer of (3.13). Then*

$$\|r(\tilde{u}^a) - (\{\theta_{op}^a, \theta_{op}^c\})\|_{\ell^*(\Lambda_a \times \Lambda_c)} \leq \|\tilde{u}^a - u^c\|_{\ell^2(\Omega_o)}. \quad (4.11)$$

Proof. We bound the approximation error directly by noting $\{\theta_{op}^a, \theta_{op}^c\}$ solves the Euler-Lagrange equation (3.16) of the reduced space problem. As a result,

$$\begin{aligned} & \|r(\tilde{u}^a) - (\{\theta_{op}^a, \theta_{op}^c\})\|_{\ell^*(\Lambda_a \times \Lambda_c)} \\ &= \sup_{\{\mu^a, \mu^c\} \neq 0} \frac{\left| \langle r(\tilde{u}^a), \{\mu^a, \mu^c\} \rangle + (u^{a,0} - u^{c,0}, v^a(\mu^a) - v^c(\mu^c))_{\ell^2(\Omega_o)} \right|}{\|\{\mu^a, \mu^c\}\|_{\ell^*(\Lambda_a \times \Lambda_c)}}. \end{aligned} \quad (4.12)$$

²This error measures the difference between traces of the true atomistic solution \tilde{u}^a and the approximate AtC solution (4.1).

Using Definition (3.14), (4.5) and (4.6), we can obtain

$$\begin{aligned}
& \langle r(\tilde{u}^a), \{\mu^a, \mu^c\} \rangle + (u^{a,0} - u^{c,0}, v^a(\mu^a) - v^c(\mu^c))_{\ell^2(\Omega_o)} \\
&= (v^a(r^a(\tilde{u}^a)) - v^c(r^c(\tilde{u}^a)), v^a(\mu^a) - v^c(\mu^c))_{\ell^2(\Omega_o)} \\
&\quad + (u^{a,0} - u^{c,0}, v^a(\mu^a) - v^c(\mu^c))_{\ell^2(\Omega_o)} \\
&= (v^a(r^a(\tilde{u}^a)) + u^{a,0} - v^c(r^c(\tilde{u}^a)) - u^{c,0}, v^a(\mu^a) - v^c(\mu^c))_{\ell^2(\Omega_o)} \\
&= (\tilde{u}^a - u^c, v^a(\mu^a) - v^c(\mu^c))_{\ell^2(\Omega_o)} \leq \|\tilde{u}^a - u^c\|_{\ell^2(\Omega_o)} \cdot \|\{\mu^a, \mu^c\}\|_{\ell^*(\Lambda_a \times \Lambda_c)}.
\end{aligned}$$

Using this identity in (4.12) completes the proof. \square

The following lemma estimates the norm of Q .

LEMMA 4.2. *Under Assumption A and Assumption B, the norm of Q is bounded by*

$$\|Q\| \lesssim \gamma^{-1} \sqrt{\frac{N}{L-K}}, \quad (4.13)$$

where the implied constant is allowed to depend on p .

Proof. Definition (4.9) implies that (4.13) will follow if we can show that

$$\|Q(\{\mu^a, \mu^c\})\|_{\ell^2(\Omega)} \lesssim \gamma^{-1} \sqrt{\frac{N}{L-K}} \|\{\mu^a, \mu^c\}\|_{\ell^*(\Lambda_a \times \Lambda_c)} \quad \forall \{\mu^a, \mu^c\} \in \Lambda_a \times \Lambda_c. \quad (4.14)$$

On the other hand, the definition of Q and (3.14) imply that (4.14) is equivalent to

$$\|v^a(\mu^a)\|_{\ell^2(\Omega_a)}^2 + \|v^c(\mu^c)\|_{\ell^2(\Omega_c/\Omega_o)}^2 \lesssim \gamma^{-2} \left(\frac{N}{L-K} \right) \|v^a(\mu^a) - v^c(\mu^c)\|_{\ell^2(\Omega_o)}^2 \quad (4.15)$$

for all $\{\mu^a, \mu^c\} \in \Lambda_a \times \Lambda_c$. To prove (4.15) we use the structure of $v^a(\mu^a)$ and $v^c(\mu^c)$.

Recall that $v^c(\mu^c) \in \mathcal{U}_c$ solves the continuum submodel

$$C_c v^c = 0 \quad \text{in } \Omega_o^\circ, \quad v_K^c = \mu_K^c, \quad v_N^c = 0.$$

It is straightforward to verify that $v^c(\mu^c)$ is a linear function, i.e.,

$$v_i^c = \alpha_c \frac{\bar{N} - i}{\bar{N} - K}, \quad (4.16)$$

where $\alpha_c = \mu_K^c$.

On the other hand, $v^a(\mu^a) \in \mathcal{U}_a$ solves the atomistic submodel

$$A_a v^a = 0 \quad \text{in } \Omega_a^\circ, \quad v_0^a = v_1^a = 0, \quad v_{L-1}^a = \mu_{L-1}^a, \quad v_L^a = \mu_L^a.$$

We decompose this field as $v^a(\mu^a) = v^1 + v^2 + v^3 + v^4$ where

$$v_i^1 = \alpha_1 \frac{i}{L} \quad \text{and} \quad v_i^2 = \alpha_2 \lambda^{L-i} \sqrt{L-K} \quad (4.17)$$

are the dominant linear and exponential modes with α_1 and α_2 determined by the boundary conditions below. Meanwhile, v^3 and v^4 are corrections to ensure that $v^a(\mu^a) = 0$ on Γ_a^- , i.e.,

$$\left\{ \begin{array}{ll} A_a v^3 = 0 & \text{in } \Omega_a^\circ \\ v^3 = -v^2 & \text{on } \Gamma_a^- \\ v^3 = 0 & \text{on } \Gamma_a^+ \end{array} \right. \quad \text{and} \quad \left\{ \begin{array}{ll} A_a v^4 = 0 & \text{in } \Omega_a^\circ \\ v^4 = -v^1 & \text{on } \Gamma_a^- \\ v^4 = 0 & \text{on } \Gamma_a^+ \end{array} \right. . \quad (4.18)$$

To obtain v^2 we need the roots of the characteristic polynomial of A_a

$$p(\sigma) = -k_2\sigma^4 - k_1\sigma^3 + (2k_1 + 2k_2)\sigma^2 - k_1\sigma - k_2,$$

which are given by (see [9])

$$\lambda_1 = \lambda_2 = 1; \quad \lambda_{3,4} = \frac{k_1 + 2k_2 \pm \sqrt{k_1^2 + 4k_1k_2}}{-2k_2}.$$

We define v^2 by setting $\lambda = \lambda_4 = \frac{k_1 + 2k_2 - \sqrt{k_1^2 + 4k_1k_2}}{-2k_2}$ in (4.17). Note that $0 < \lambda < 1$, as seen from the assumptions $k_1 > 0$, $k_2 < 0$, and $k_1 + 4k_2 > 0$.

The coefficients α_1 and α_2 are uniquely determined from the boundary condition $v^a(\mu^a) = \mu^a$ on Γ_a^+ , which yields the following 2×2 system:

$$\begin{aligned} \left(1 - \frac{1}{L}\right) \alpha_1 + \lambda \sqrt{L-K} \alpha_2 &= \mu_{L-1}^a, \\ \alpha_1 + \sqrt{L-K} \alpha_2 &= \mu_L^a. \end{aligned} \quad (4.19)$$

Recall that $\alpha_c = \mu_K^c$. In the following, we define

$$\alpha := \sqrt{\alpha_1^2 + \alpha_2^2 + \alpha_c^2}.$$

According to Remark 3.1, the result of Lemma 3.1 applies to v^3 and v^4 , and so,

$$\|v^3\|_{\ell^2(\Omega_a)}^2 \lesssim L \|v^2\|_{\ell^2(\Gamma_a^-)}^2 \quad \text{and} \quad \|v^4\|_{\ell^2(\Omega_a)}^2 \lesssim L \|v^1\|_{\ell^2(\Gamma_a^-)}^2.$$

Since $v^1|_{\Gamma_a^-} = (0, \alpha_1/L)$ and $v^2|_{\Gamma_a^-} = \alpha_2 \sqrt{L-K} (\lambda^L, \lambda^{L-1})$, we have the bounds

$$\|v^3\|_{\ell^2(\Omega_0)}^2 \lesssim \lambda^{2(L-1)} L(L-K) \alpha_2^2, \quad \text{and} \quad \|v^4\|_{\ell^2(\Omega_0)}^2 \lesssim L \frac{\alpha_1^2}{L^2}. \quad (4.20)$$

Using (4.20) yields the following lower bound for the right hand side in (4.15):

$$\begin{aligned} \|v^a(\mu^a) - v^c(\mu^c)\|_{\ell^2(\Omega_0)} &\geq \|v^1 + v^2 - v^c\|_{\ell^2(\Omega_0)} - \|v^3\|_{\ell^2(\Omega_0)} - \|v^4\|_{\ell^2(\Omega_0)} \\ &\gtrsim \|v^1 + v^2 - v^c\|_{\ell^2(\Omega_0)} - \left(\lambda^{L-1} \sqrt{L(L-K)} + \frac{1}{\sqrt{L}} \right) \alpha. \end{aligned} \quad (4.21)$$

We proceed with estimating

$$\|v^1 + v^2 - v^c\|_{\ell^2(\Omega_0)}^2 = \|v^1 - v^c\|_{\ell^2(\Omega_0)}^2 + 2(v^1 - v^c, v^2)_{\ell^2(\Omega_0)} + \|v^2\|_{\ell^2(\Omega_0)}^2. \quad (4.22)$$

The term $\|v^1 - v^c\|_{\ell^2(\Omega_0)}^2$ is similar to the term in (3.14) defining the trace norm $\|\cdot\|_{\ell^*(\Lambda_a \times \Lambda_c)}$, but it is simpler in that both v^1 and v^c solve continuum problems. We will prove in Appendix B that

$$\|v^1 - v^c\|_{\ell^2(\Omega_0)}^2 \gtrsim (L-K) \gamma^2 (\alpha_c^2 + \alpha_1^2) \quad (4.23)$$

for large N . Furthermore, summing a finite geometric series shows

$$\|v^2\|_{\ell^2(\Omega_0)}^2 = \frac{L-K}{1-\lambda^2} \left(1 - \lambda^{2(L-K+1)}\right) \alpha_2^2. \quad (4.24)$$

Intuitively, one should suspect the cross term, $(v^1 - v^c, v^2)_{\ell^2(\Omega_0)}$, in (4.22) to be estimable for large overlap widths since the exponential term v^2 is not well approximated by any linear function. We now calculate via explicit summation that

$$\begin{aligned}
(v^1 - v^c, v^2)_{\ell^2(\Omega_0)} &= \sum_{i=K}^L \left(\alpha_1 \frac{i}{L} - \alpha_c \frac{\bar{N} - i}{\bar{N} - K} \right) \alpha_2 \lambda^{L-i} \sqrt{L - K} \\
&= \alpha_2 \sqrt{L - K} \left(\alpha_1 \sum_{i=K}^L \frac{i}{L} \lambda^{L-i} - \alpha_c \sum_{i=K}^L \frac{\bar{N} - i}{\bar{N} - K} \lambda^{L-i} \right) \\
&\geq -|\alpha_1 \alpha_2| \sqrt{L - K} \sum_{i=K}^L \lambda^{L-i} - |\alpha_c \alpha_2| \sqrt{L - K} \sum_{i=K}^L \lambda^{L-i} \\
&\gtrsim -\sqrt{L - K} \left(\frac{1 - \lambda^{L-K+1}}{1 - \lambda} \right) \alpha^2.
\end{aligned} \tag{4.25}$$

Using the inequalities (4.23), (4.24), and (4.25) in (4.22) produces

$$\begin{aligned}
\|v^1 + v^2 - v^c\|_{\ell^2(\Omega_0)}^2 &\gtrsim (L - K) \gamma^2 (\alpha_c^2 + \alpha_1^2) \\
&\quad + (L - K) \left(\frac{1 - \lambda^{2(L-K+1)}}{1 - \lambda^2} \right) \alpha_2^2 - \sqrt{L - K} \left(\frac{1 - \lambda^{L-K+1}}{1 - \lambda} \right) \alpha^2 \\
&= (L - K) \left[\left(\gamma^2 - \frac{1}{\sqrt{L - K}} \cdot \frac{1 - \lambda^{L-K+1}}{1 - \lambda} \right) (\alpha_c^2 + \alpha_1^2) \right. \\
&\quad \left. + \left(\frac{1 - \lambda^{2(L-K+1)}}{1 - \lambda^2} - \frac{1}{\sqrt{L - K}} \cdot \frac{1 - \lambda^{L-K+1}}{1 - \lambda} \right) \alpha_2^2 \right].
\end{aligned} \tag{4.26}$$

For a sufficiently large overlap region, there holds

$$\sqrt{L - K} > \max \left\{ \frac{1 - \lambda^{L-K+1}}{\gamma^2(1 - \lambda)}, \frac{1 + \lambda}{1 + \lambda^{L-K+1}} \right\},$$

which guarantees the positivity of the terms multiplying $\alpha_c^2 + \alpha_1^2$ and α_2^2 above. Then since $\gamma^2 < 1$, we obtain from (4.26) that

$$\|v^1 + v^2 - v^c\|_{\ell^2(\Omega_0)}^2 \gtrsim (L - K) \gamma^2 \alpha^2. \tag{4.27}$$

Similarly, using (4.27) in (4.21) yields

$$\|v^a - v^c\|_{\ell^2(\Omega_0)} \gtrsim \sqrt{L - K} \gamma \alpha. \tag{4.28}$$

To complete the proof, we use the above results to estimate the left-hand side in (4.15):

$$\begin{aligned}
\|v^a\|_{\ell^2(\Omega_a)}^2 + \|v^c\|_{\ell^2(\Omega_c \setminus \Omega_o)}^2 &= \|v^1 + v^2 + v^3 + v^4\|_{\ell^2(\Omega_a)}^2 + \|v^c\|_{\ell^2(\Omega_c \setminus \Omega_o)}^2 \\
&\leq 4 \left(\|v^1\|_{\ell^2(\Omega_a)}^2 + \|v^2\|_{\ell^2(\Omega_a)}^2 + \|v^3\|_{\ell^2(\Omega_a)}^2 + \|v^4\|_{\ell^2(\Omega_a)}^2 \right) + \|v^c\|_{\ell^2(\Omega_c \setminus \Omega_o)}^2 \\
&\leq 4 \left(L \alpha_1^2 + (L - K) \frac{1 - \lambda^{2(1+L-K)}}{1 - \lambda^2} \alpha_2^2 + L(L - K) \lambda^{2L-2} \alpha_2^2 + \frac{\alpha_1^2}{L} \right) \\
&\quad + (\bar{N} - L) \alpha_c^2 \\
&\lesssim N(\alpha_c^2 + \alpha_1^2 + \alpha_2^2) \\
&\lesssim \frac{N \gamma^{-2}}{L - K} \|v^a - v^c\|_{\ell^2(\Omega_0)}^2.
\end{aligned}$$

Estimates of the norms of v^1 , v^2 , v^3 , v^4 , and v^c follow from (3.12) in Lemma 3.1, (4.24) and (4.20), respectively. The final inequality, which establishes the assertion of the lemma, is a consequence of (4.28). \square

All results necessary for the completion of the AtC approximation error bound in (4.8) are now in place.

PROPOSITION 4.1. *Let \tilde{u}^a solve (2.6) and $\{\theta_{op}^a, \theta_{op}^c\}$ be the minimizer of (3.13). The AtC solution satisfies the error bound*

$$\|\tilde{u}^a - u^{atc}\|_{\ell^2(\Omega)} \lesssim \left(1 + \gamma^{-1} \sqrt{\frac{N}{L-K}}\right) \|\tilde{u}^a - u^c\|_{\ell^2(\Omega_c)}. \quad (4.29)$$

Proof. Recall the split of the AtC solution error into a consistency error due to P and the approximation error in the reduced space problem (3.13):

$$\begin{aligned} \|\tilde{u}^a - u^{atc}\|_{\ell^2(\Omega)} &= \|\tilde{u}^a - P(\{\theta_{op}^a, \theta_{op}^c\})\|_{\ell^2(\Omega)} \\ &\leq \|\tilde{u}^a - P(r(\tilde{u}^a))\|_{\ell^2(\Omega)} + \|Q\| \cdot \|r(\tilde{u}^a) - \{\theta_{op}^a, \theta_{op}^c\}\|_{\ell^*(\Lambda_a \times \Lambda_c)}, \end{aligned}$$

Using (4.10) for the consistency error, (4.11) for the approximation error, and (4.13) for operator norm yields the result of the proposition. \square

Proposition 4.1 reveals that the accuracy of the AtC approximation is determined by two independent factors. Replacing the atomistic model with a continuum model on Ω_c introduces the *continuum modeling error* $\|\tilde{u}^a - u^c\|_{\ell^2(\Omega_c)}$, which is independent of the choice of the coupling mechanism. An inherent assumption in atomistic-to-continuum coupling is that the continuum model closely approximates the atomistic model in the continuum region, which can be expected when there are no defects in the continuum region [18]. Thus, we expect $\|\tilde{u}^a - u^c\|_{\ell^2(\Omega_c)}$ to be small so long as this assumption holds. On the other hand, the coupling mechanism via the optimization framework introduces the prefactor

$$\sqrt{\frac{N}{L-K}} \approx \sqrt{\frac{|\Omega|}{|\Omega_o|}},$$

which depends on the size of the overlap region. As can be expected, the AtC error is inversely proportional to the size of Ω_o .

We can precisely estimate the modeling error by applying the estimate (2.16) to the domain Ω_c . The operator C is now the 1D discrete Laplacian on Ω_c with homogeneous Dirichlet boundary conditions at K and $N-1$. Thus, the minimum eigenvalue for C is $\lambda_1 = 4k_c \sin^2\left(\frac{\pi}{2(n+1)}\right)$ where now $n = N-K-2$ is the dimension of C . We then have since $\tilde{u}^a - u^c = 0$ at atoms K and $N-1$ that

$$\|\tilde{u}^a - u^c\|_{\ell^2(\Omega_c)} \lesssim (N-K)^2 \|\Delta_1^2 \tilde{u}^a\|_{\ell^2(\Omega_c)}. \quad (4.30)$$

The estimate (4.30) confirms that the modeling error is small whenever \tilde{u}^a is smooth over the continuum region in the sense that $\|\Delta_1^2 \tilde{u}^a\|_{\ell^2(\Omega_c)}$ is small.

By using the modeling error bound (4.30) in (4.29), we obtain the following theorem for the AtC error estimate.

THEOREM 4.2. *Under the conditions of Assumptions A and B, let \tilde{u}^a solve (2.6), and let $\{\theta_{op}^a, \theta_{op}^c\}$ be the minimizer of (3.13). Then*

$$\|\tilde{u}^a - u^{atc}\|_{\ell^2(\Omega)} \lesssim \left(1 + \gamma^{-1} \sqrt{\frac{N}{L-K}}\right) (N-K)^2 \|\Delta_1^2 \tilde{u}^a\|_{\ell^2(\Omega_c)}, \quad (4.31)$$

where $u^{atc} = P(\{\theta_{op}^a, \theta_{op}^c\})$ is the AtC solution and P is defined by (4.2).

Note that the dependence of the AtC error on the size of the overlap domain is unchanged, i.e., as the overlap width is increased, the error decreases. In the present situation, we did not coarse-grain the continuum region, so the only increase in complexity comes from increasing the size of the atomistic and continuum regions.

Thermodynamic limit. By letting $N \rightarrow \infty$, the problem above is an example of a thermodynamic limit. A further estimate would typically be obtained by assuming the fully atomistic solution decays sufficiently rapidly as $N \rightarrow \infty$. See [18] for an analysis in this setting for quasicontinuum methods.

We may conversely introduce an interatomic spacing parameter ϵ with ϵ dependent norm

$$\|u\|_\epsilon = \sqrt{\epsilon \sum u_i^2}.$$

Setting $\epsilon = N^{-1}$ maintains $\Omega = [0, 1]$ and scaling the lattice by $j \mapsto \epsilon j$ scales

$$\|\Delta_1^2 u\|_{\ell^2(\Omega_c)} \mapsto \epsilon^4 \|\Delta_1^2 u\|_{\ell^2(\Omega_c), \epsilon}.$$

The estimate in (4.31) under this scaling is

$$\|\tilde{u}^a - u^{atc}\|_{\ell^2(\Omega), \epsilon} \lesssim \frac{\epsilon^{\frac{3}{2}}}{\sqrt{L-K}} \|\Delta_1^2 \tilde{u}^a\|_{\ell^2(\Omega_c), \epsilon}, \quad (4.32)$$

which is the scaling limit as $\epsilon \rightarrow 0$. See [11] for the derivation of a similar estimate in the case of the force based quasicontinuum operator in which ϵ is maintained as a parameter throughout. Recalling Assumptions A and B, if the overlap region Ω_o has width $|\Omega_o| := (L-K)\epsilon^{1/p}$ in the scaling limit, then we obtain the bound

$$\|\tilde{u}^a - u^{atc}\|_{\ell^2(\Omega), \epsilon} \lesssim \frac{\epsilon^{\frac{3}{2} + \frac{1}{2p}}}{|\Omega_o|^{\frac{1}{2}}} \|\Delta_1^2 \tilde{u}^a\|_{\ell^2(\Omega_c), \epsilon}. \quad (4.33)$$

Hence, we may achieve any power of ϵ in the interval $(\frac{3}{2}, 2)$ for $p > 1$.

5. Conclusion. This paper formulates and analyzes a new, optimization-based strategy for atomistic-to-continuum coupling. Specifically, we pose the problem of coupling a non-local, atomistic description of a material with a local, continuous description as a constrained optimization problem. The objective is to minimize the ℓ^2 difference between the continuum and atomistic displacement fields over an overlap region, subject to constraints expressing the atomistic and continuum force balances in the respective subregions. The traces of the atomistic and continuum solution components on the boundary of the overlap region act as virtual boundary controls. Thus, our approach can be viewed as an extension of the heterogeneous decomposition method [12] to the AtC context.

Acknowledgments. The work of P. Bochev was supported by the Applied Mathematics Program within the Department of Energy (DOE) Office of Advanced Scientific Computing Research (ASCR). Part of this research was carried under the auspices of the Collaboratory on Mathematics for Mesoscopic Modeling of Materials (CM4). The work of D. Olson was partially supported by Sandia's Computer Science Research Institute Summer Internship Program.

Appendix A. Stability of atomistic and continuum problems. In this appendix, we prove the result stated in Lemma 3.1:

$$\begin{aligned} \|v^a(\theta^a)\|_{\ell^2(\Omega_a)}^2 &\lesssim L\|\theta^a\|_{\ell^2(\Gamma_a^+)}^2, \\ \|v^c(\theta^c)\|_{\ell^2(\Omega_c)}^2 &\leq (N-K)\|\theta^c\|_{\ell^2(\Gamma_c^-)}^2. \end{aligned} \quad (\text{A.1})$$

The second bound is a direct consequence of the maximum principle for the continuum operator $C = -k_c\Delta_1$. Recalling that $v^c(\theta^c)$ is zero on Γ_c^+ and equal to θ_K^c on $\Gamma_c^- = \{K\}$, we have

$$\|v^c(\theta^c)\|_{\ell^2(\Omega_c)}^2 = \sum_{i=K}^{N-1} (v_i^c)^2 \leq \sum_{i=K}^{N-1} (\theta_K^c)^2 = (N-K)(\theta_K^c)^2. \quad (\text{A.2})$$

To prove the first bound in (A.1), we note that the atomistic solution, $v^a(\theta^a)$, may be written as

$$\begin{aligned} v^a(\theta^a)_n &= \beta_1 \frac{n}{L} + \beta_2 \frac{L-n}{L} + \beta_3 \lambda^n + \beta_4 \lambda^{L-n} \\ &=: \beta_1 v^1(\theta^a) + \beta_2 v^2(\theta^a) + \beta_3 v^3(\theta^a) + \beta_4 v^4(\theta^a), \end{aligned} \quad (\text{A.3})$$

where $0 < \lambda < 1$ was defined in Lemma 4.2 and the coefficients are determined via the boundary conditions $v^a(\theta^a) = 0$ on Γ_a^- and $v^a(\theta^a) = \theta^a$ on Γ_a^+ . Specifically,

$$T_L \begin{pmatrix} \beta_1 \\ \beta_2 \\ \beta_3 \\ \beta_4 \end{pmatrix} := \begin{pmatrix} 0 & 1 & 1 & \lambda^L \\ \frac{1}{L} & \frac{L-1}{L} & \lambda & \lambda^{L-1} \\ \frac{L-1}{L} & \frac{1}{L} & \lambda^{L-1} & \lambda \\ 1 & 0 & \lambda^L & 1 \end{pmatrix} \begin{pmatrix} \beta_1 \\ \beta_2 \\ \beta_3 \\ \beta_4 \end{pmatrix} = \begin{pmatrix} 0 \\ 0 \\ \theta_{L-1}^a \\ \theta_L^a \end{pmatrix}, \quad (\text{A.4})$$

where

$$T_L \rightarrow \begin{pmatrix} 0 & 1 & 1 & 0 \\ 0 & 1 & \lambda & 0 \\ 1 & 0 & 0 & \lambda \\ 1 & 0 & 0 & 1 \end{pmatrix} =: T \text{ as } L \rightarrow \infty. \quad (\text{A.5})$$

For any $\delta > 0$, we can therefore choose L such that $\|T_L^{-1}\| < \|T^{-1}\| + \delta$, and hence

$$(\beta_1^2 + \beta_2^2 + \beta_3^2 + \beta_4^2) \leq (\|T^{-1}\| + \delta)^2 \left((\theta_{L-1}^a)^2 + (\theta_L^a)^2 \right). \quad (\text{A.6})$$

Using successive Cauchy inequalities and explicit summation of finite geometric series yields

$$\begin{aligned} \|v^a(\theta^a)\|_{\ell^2(\Omega_a)}^2 &\leq 4 \left(\beta_1^2 \|v^1(\theta^a)\|_{\ell^2(\Omega_a)}^2 + \beta_2^2 \|v^2(\theta^a)\|_{\ell^2(\Omega_a)}^2 + \beta_3^2 \|v^3(\theta^a)\|_{\ell^2(\Omega_a)}^2 + \beta_4^2 \|v^4(\theta^a)\|_{\ell^2(\Omega_a)}^2 \right) \\ &\lesssim 4 \left(\beta_1^2 L + \beta_2^2 L + \beta_3^2 \left(\frac{1 - \lambda^{L+1}}{1 - \lambda} \right) + \beta_4^2 \left(\frac{\lambda^{-1} - \lambda^L}{\lambda^{-1} - 1} \right) \right) \\ &\lesssim L (\beta_1^2 + \beta_2^2 + \beta_3^2 + \beta_4^2) \\ &\leq (\|T^{-1}\| + \delta)^2 L \left((\theta_{L-1}^a)^2 + (\theta_L^a)^2 \right), \end{aligned}$$

for large enough L by (A.6).

Appendix B. Estimate of $\|v^1 - v^c\|_{\ell^2(\Omega_0)}$. Finally, we establish the estimate (4.23) under the conditions of Assumptions A and B. Recall that v^c and v^1 are defined in (4.16) and (4.17), respectively, and so,

$$\|v^c - v^1\|_{\ell^2(\Omega_0)}^2 = \sum_{i=K}^L \left(\alpha_c \frac{\bar{N} - i}{\bar{N} - K} - \alpha_1 \frac{i}{L} \right)^2 = \tilde{A}\alpha_c^2 - 2\tilde{C}\alpha_c\alpha_1 + \tilde{B}\alpha_1^2 \quad (\text{B.1})$$

where the coefficients of the quadratic form in (B.1) are given by

$$\tilde{A} = \sum_{i=K}^L \left(\frac{\bar{N} - i}{\bar{N} - K} \right)^2, \quad \tilde{B} = \sum_{i=K}^L \left(\frac{i}{L} \right)^2, \quad \text{and} \quad \tilde{C} = \sum_{i=K}^L \left(\frac{\bar{N} - i}{\bar{N} - K} \right) \cdot \left(\frac{i}{L} \right),$$

respectively. Summing the finite series for each coefficient yields $\tilde{A} = \beta \cdot A$, $\tilde{B} = \beta \cdot B$, and $\tilde{C} = \beta \cdot C$ where the common factor is $\beta = (1 + L - K)$ and

$$\begin{aligned} A &= \frac{6\bar{N}^2 + 2L^2 + 2K^2 - 6K\bar{N} - 6L\bar{N} + 2KL + L - K}{6(K - \bar{N})^2}, \\ B &= \frac{2L^2 + 2K^2 + 2KL + L - K}{6L^2}, \\ C &= \frac{2L^2 + 2K^2 + 2KL - 3K\bar{N} - 3L\bar{N} + L - K}{6L(K - \bar{N})}, \end{aligned}$$

respectively. Using that $K = (1 - \gamma)L$ allows us to further write the coefficients as

$$\begin{aligned} A &= \frac{\bar{N}^2 + L^2(1 - \gamma + \frac{1}{3}\gamma^2) + \frac{1}{6}\gamma L - L\bar{N}(2 - \gamma)}{(\bar{N} - (1 - \gamma)L)^2}, \\ B &= \frac{L(1 - \gamma + \frac{1}{3}\gamma^2) + \frac{1}{6}\gamma}{L}, \quad \text{and} \quad C = \frac{\bar{N}(1 - \frac{1}{2}\gamma) - \frac{1}{6}\gamma - L(1 - \gamma + \frac{1}{3}\gamma^3)}{\bar{N} - (1 - \gamma)L}. \end{aligned}$$

Assumption A implies that $\lim_{N \rightarrow \infty} L/N = 0$, and so

$$A \rightarrow A_\infty = 1, \quad B \rightarrow B_\infty = 1 - \gamma + \frac{1}{3}\gamma^2, \quad \text{and} \quad C \rightarrow C_\infty = 1 - \frac{1}{2}\gamma.$$

Let $0 \leq \lambda_1 \leq \lambda_2$ be the eigenvalues of the quadratic form $A_\infty\alpha_c^2 - 2C_\infty\alpha_c\alpha_1 + B_\infty\alpha_1^2$. Using the expressions for the determinant and the trace of the quadratic form, $\lambda_1\lambda_2 = A_\infty B_\infty - C_\infty^2$ and $\lambda_1 + \lambda_2 = A_\infty + B_\infty$, we can estimate

$$\lambda_1 = \frac{\lambda_1\lambda_2}{\lambda_2} \geq \frac{\lambda_1\lambda_2}{\lambda_1 + \lambda_2} = \frac{\frac{1}{12}\gamma^2}{1 + (1 - \gamma + \frac{1}{3}\gamma^2)} \geq \frac{1}{24}\gamma^2.$$

This completes the proof.

REFERENCES

- [1] S. Badia, M. Parks, P. Bochev, M. Gunzburger, and R. Lehoucq. On atomistic-to-continuum coupling by blending. *Multiscale Modeling & Simulation*, 7(1):381–406, 2008.
- [2] P. Bauman, H. Ben Dhia, N. Elkhodja, J. Oden, and S. Prudhomme. On the application of the Arlequin method to the coupling of particle and continuum models. *Computational Mechanics*, 42:511–530, 2008. 10.1007/s00466-008-0291-1.
- [3] P. Bochev and D. Ridzal. Additive operator decomposition and optimization-based reconnection with applications. In I. Lirkov, S. Margenov, and J. Wasniewski, editors, *Proceedings of LSSC 2009*, volume 5910 of *Springer Lecture Notes in Computer Science*, 2009.
- [4] P. Bochev and D. Ridzal. An optimization-based approach for the design of PDE solution algorithms. *SIAM Journal on Numerical Analysis*, 47(5):3938–3955, 2009.
- [5] P. Bochev, D. Ridzal, and D. Young. Optimization-based modeling with applications to transport. Part 1. Abstract formulation. In I. Lirkov, S. Margenov, and J. Wasniewski, editors, *Proceedings of LSSC 2011*, Springer Lecture Notes in Computer Science, Submitted 2011.
- [6] F. Brezzi. On the existence, uniqueness and approximation of saddle-point problems arising from lagrangian multipliers. *RAIRO Anal. Numer*, 8(2):129–151, 1974.
- [7] L. Chamoin, S. Prudhomme, H. Ben Dhia, and J. Oden. Ghost forces and spurious effects in atomic-to-continuum coupling methods by the Arlequin approach. *International Journal for Numerical Methods in Engineering*, 83(8-9):1081–1113, 2010.
- [8] W. Curtin and R. Miller. Atomistic/continuum coupling in computational materials science. *Modelling Simul. Mater. Sci. Eng.*, 11:R33–R68, 2003.
- [9] M. Dobson and M. Luskin. An analysis of the effect of ghost force oscillation on quasicontinuum error. *Mathematical Modelling and Numerical Analysis*, 43:591–604, 2009.
- [10] M. Dobson, M. Luskin, and C. Ortner. Accuracy of quasicontinuum approximations near instabilities. *Journal of the Mechanics and Physics of Solids*, 58:1741–1757, 2010.
- [11] M. Dobson, M. Luskin, and C. Ortner. Stability, instability, and error of the force-based quasicontinuum approximation. *Archive for Rational Mechanics and Analysis*, 197(1):179–202, 2010.
- [12] P. Gervasio, J.L. Lions, and A. Quarteroni. Heterogeneous coupling by virtual control methods. *Numerische Mathematik*, 90(2):241–264, 2001.
- [13] B. Van Koten and M. Luskin. Analysis of energy-based blended quasi-continuum approximations. *SIAM J. Numer. Anal.*, 49(5):2182–2209, 2011.
- [14] X. Li, M. Luskin, and C. Ortner. Positive-definiteness of the blended force-based quasicontinuum method. *SIAM J. Multiscale Modeling & Simulation*, 10, 2012. arXiv:1112.2528v1.
- [15] J.L. Lions. Virtual and effective control for distributed systems and decomposition of everything. *Journal d’Analyse Mathématique*, 80:257–297, 2000. 10.1007/BF02791538.
- [16] J.L. Lions and O. Pironneau. Virtual control, replicas and decomposition of operators. *C. R. Acad. Sci. Paris*, 330(1):47–54, 2000.
- [17] M. Luskin, C. Ortner, and B. Van Koten. Formulation and optimization of the energy-based blended quasicontinuum method. *Computer Methods in Applied Mechanics and Engineering*, 253:160–168, 2013. arXiv: 1112.2377.
- [18] Mitchell Luskin and Christoph Ortner. Atomistic-to-continuum coupling. *Acta Numerica*, 22:397–508, 2013.
- [19] M. Parks, P. Bochev, and R. Lehoucq. Connecting atomistic-to-continuum coupling and domain decomposition. *SIAM J. Multiscale Model. Simul.*, 7(1):362–380, 2008.
- [20] V. B. Shenoy, R. Miller, E. B. Tadmor, D. Rodney, R. Phillips, and M. Ortiz. An adaptive finite element approach to atomic-scale mechanics—the quasicontinuum method. *J. Mech. Phys. Solids*, 47(3):611–642, 1999.